Bull. Mater. Sci., Vol. 37, No. 5, August 2014, pp. 1167–1174. © Indian Academy of Sciences.

Magnetic-supported cucurbituril: A recyclable adsorbent for the removal of humic acid from simulated water

QIN YANG*, YING JIANG, XIAOLI LI, YONGLI YANG and LIYUN HU

Department of Chemistry, School of Science, Xi'an University of Architecture and Technology, Xi'an 710055, China

MS received 19 May 2013; revised 4 July 2013

Abstract. Magnetic cucurbituril (MQ[*n*]), a new functional material compound, was prepared via chemical co-precipitation method as a high-capacity adsorbent for humic acid (HA). The material was characterized by X-ray diffraction (XRD), scanning electron microscopy (SEM), Fourier transform infrared spectroscopy (FT–IR) and thermal gravimetric analysis (TGA), respectively, indicating that Q[*n*] has been grafted on the surface of Fe_3O_4. Its adsorption–desorption behaviour towards HA from aqueous solution have been investigated. MQ[*n*] demonstrated good adsorption capacity at pH 7 in adsorption experiments. Adsorption isotherm could be well interpreted by the Freundlich isotherm model. Adsorption kinetic followed pseudo-second-order kinetics, which indicated that the limit factor of adsorption HA was adsorption mechanism. The negative value of thermodynamic parameters showed that adsorption process was spontaneous and exothermic. Moreover, the capacity of MQ[*n*] was also above 80% after being used for four times, so it may have potential industrial applications.

Keywords. Cucurbituril; magnetic; adsorption; humic acid; kinetics.

1. Introduction

Humic acid (HA), a mixture of stable, weak and alkaline natural polymers that resides as a predominant type of organics in natural waters (Baker and Khalili 2004), can react with chloric disinfectant of drinking water to produce by-products such as trihalomethane and haloacetic acids, which are known to be carcinogenic, teratogenic and mutagenic to human health. In the mean time, it can form complexes with heavy metals and pesticides, enhancing the material durability and biological accumulation (Domany *et al* 2002). Therefore, it is necessary to remove HA from wastewater. At present, a variety of methods including ultrafiltration, coagulation, biodegradation, ozonation and adsorption have been applied for removal of HA from wastewater (Latifoglu and Gurol 2003; Seredynska-Sobecka 2006; Senem *et al* 2007; Tang *et al* 2007; Ji *et al* 2008). Among them, adsorption has been paid close attention since it is simple, environmentally friendly and cost-effective (Koparal *et al* 2008). The commonly used adsorbents are activated carbon (Deng and Bai 2004), fly ash (Wang and Zhu 2007), chitosan (Anirudhan *et al* 2008), resin (Zhao *et al* 2008), polypropylene fiber membrane (Wang *et al* 2010) and polypyrrole (Bai and Zhang 2001).

Cucurbituril (Q[*n*]), a family of macrocyclic host molecules, possessing its unique structure of centre hydrophobic cavity and hydrophilic portals that can form stable clathrate compounds with guest molecules through van der Waals interaction (Peerannawar *et al* 2012), hydrophobic interaction (Feng *et al* 2009), electrostatic interaction (Buschmann *et al* 2000), hydrogen bonding (Karcher *et al* 2001a), ion–dipole (Buschmann *et al* 2006) or dipole–dipole interaction (Wei *et al* 2005; Zhang *et al* 2008). Q[5–8] are of the same height (9·1 Å); however, they all differ in the diameter of their carbonyl portals and cavities, which are 2·4–6·9 Å and 4·4–8·8 Å, respectively (Petrov *et al* 2009; Saleh *et al* 2011). In addition, Q[*n*] is practically insoluble in all common organic solvents. The solubility in water given in the literature varies between 13 and 20 mmol L^{-1} (Karcher *et al* 2001a). Q[*n*] has other advantages such as its strong rigid structure, stable chemical property and low toxicity (Wheate 2008). Therefore, Q[*n*] is considered as a promising functional material compounds with extensive applications in various fields, such as biomedicine, materials science, pharmacology and water treatment. Buschmann and Schollmeye (1993) found that Q[6] has high selectivity and capture ability for many ions, such as Cr and Cu in dye wastewater under the condition of high acidity. Therefore, it can be used in wastewater treatment. However, Lim *et al* (2008) applied Q[6] to water treatment and found that Q[6] can load more than 1 $g \cdot g^{-1}$ in

*Author for correspondence (yangjiaxin929@163.com)

appropriate conditions, but if the concentration and acidity of metal ions in the solution are too high, Q[6] will be dissolved and the amount of adsorption decreased. Furthermore, Q[*n*] was used as adsorbent to remove the reactive dye of printing and dyeing wastewater by Karcher *et al* (1999, 2001b) and exhibited high adsorption efficiency. But in the authentic printing and dyeing wastewater treatment, Q[*n*] was dissolved at least 20% and even cucurbituril precipitated on silica was partly dissolved, thus, inappropriate for printing and dyeing wastewater treatment. In addition, German scientists, Karcher *et al* (2001b), utilized chemical ozonation to dispose Q[*n*], which has adsorbed other molecules, but unfortunately, dissolved Q[*n*] was oxidated by ozone; thus, producing nitrite, nitrate, formic acid salt, acetate and oxalic acid salt, so that chemical oxygen demand (COD) content was too high to treat water in the recovery process. Our team has found good removal efficiency of HA adsorbed by Q[*n*], but we also encountered the problems mentioned earlier (Yang *et al* 2012). Therefore, it is important to seek a suitable support material applying to wastewater treatment system without losing the relevant properties.

Recently, magnetic carrier methods have been widely used in the processes of the separation of biological cells, coal desulphurization and the treatment of wastewater due to their magnetic properties, chemical stability, low toxicity and adsorption capacity, ease in synthesis and excellent recycling capability (Parsonage 1992). Not only does MQ[*n*] have stable structure and higher adsorption capacity, but also it is easily separated from wastewater. In this work, MQ[*n*] were prepared by chemical co-precipitation method and its morphology and structure was characterized. Adsorption and desorption behaviours of this interesting composite material were studied for HA in simulated water.

2. Experimental

2.1 *Materials*

Cucurbituril (Q[*n*]) was prepared and purified following traditional method (Bardelang *et al* 2007). Ferrous ammonium sulfate hexahydrate ($(NH_4)_2Fe(SO_4)_2{\cdot}6H_2O$), ammonium ferric sulfate dodecahydrate ($(NH_4)Fe(SO_4)_3{\cdot}12H_2O$), ammonia, anhydrous ethanol were purchased from Kemiou Chemical Agent Company (TianJin, China). Humic acid (HA) was supplied by JvFen Chemical Agent Company (ShangHai, China). All other reagents used in this study were analytical grade.

2.2 *Preparation of MQ[n]*

As much as 1·5 g of Q[*n*], 1·7 g of $(NH_4)_2Fe(SO_4)_2{\cdot}6H_2O$ and 2·51 g of $(NH_4)Fe(SO_4)_3{\cdot}12H_2O$ were dissolved in 200 mL of deionized water. The suspension was sonicated for 10 min. A total of 10 mL of 8 mol L^{-1} $NH_3{\cdot}H_2O$ was added dropwise after the solution was heated to 50 °C with vigorous stirring at a speed of 1000 rpm in the presence of nitrogen. The pH was maintained at 11–12 during the whole reaction. After finishing the reaction, the precipitate was isolated from suspension by magnets, washed three times with anhydrous ethanol and deionized water, and dried in a vacuum oven at 60 °C.

2.3 *Characterization*

The X-ray powder diffraction (XRD) pattern was recorded by an X-ray diffractometer (Bruker, German) using CuKα radiation. The size and morphology of the samples were observed by scanning electron microscopy (S-570, Japan Hitachi). FT–IR measurements were performed by Fourier transform infrared spectrophotometer (Shimadzu IR-21, Japan) using KBr background in the range of 400–4000 cm^{-1}. Thermal gravimetric analysis was conducted with METTLER TGA/DSC 1 STAR System thermal analyzer (Switzerland) at a heating rate of 10 °C min^{-1} in a nitrogen atmosphere.

2.4 *Adsorption/desorption studies*

The effect of pH on the HA removal by MQ[*n*] was conducted by adding 0·02 g of MQ[*n*] to 20 mL of HA solution (10 mg L^{-1}). The initial pH of HA solution was adjusted by 0·1 mol L^{-1} HCI and NaOH ranging from 2 to 14. After 12 h, the liquid supernatant was measured at the maximum wavelength (254 nm) by UV–Vis spectrophotometer (Thermo, USA).

Adsorption experiments were carried out in a set of beakers containing 20 mL of HA solution at different concentrations ranging from 2 to 15 mg L^{-1}. To each beaker, pH was adjusted to 7, 0·02 g MQ[*n*] was added and temperature was maintained at 25, 35 and 45 °C for 12 h. The concentration of the residual HA was measured by UV–Vis spectrophotometer. The amount of HA adsorbed on MQ[*n*] was calculated by the following equation (Samiey and Toosi 2010)

$$Q_e = (C_0 - C_e)V/M, \quad (1)$$

where Q_e is the amount of adsorbed HA on a unit mass of MQ[*n*] (mg g^{-1}); C_0 and C_e are the initial concentration and equilibrium concentration of HA, respectively (mg L^{-1}); V the volume of HA solution (L) and M the mass of MQ[*n*] (g). The standard curve of HA is $Y = -0{\cdot}00107 + 0{\cdot}03642 \times X$, $R^2 = 0{\cdot}9996$.

For the kinetic experiment, 0·02 g of MQ[*n*] was added into different concentrations of the HA solution at 25 °C. The pH was adjusted to 7. At different time intervals, the remaining amount of HA in supernatant was determined using UV–Vis spectrophotometer. The adsorption amount was calculated according to (1).

Desorption experiments were conducted by adding 0·02 g of MQ[*n*] to 20 mL of (10 mg L^{-1}) HA solution at pH 7 for 12 h. Aqueous samples were collected for further analysis. The MQ[*n*] was separated from the solution using magnets and washed with 2 mol L^{-1} NaOH and deionized water until the pH was 7. Subsequently, the MQ[*n*] was used to remove the same concentration of HA solution again. The process was repeated four times.

3. Results and discussion

3.1 *Characterization of MQ[n]*

Figure 1 shows the XRD patterns of Q[*n*] and MQ[*n*]. For the XRD patterns of Q[*n*], there is a small hump ($2\theta = 23$) corresponding to amorphous Q[*n*]. However, all the characteristic peaks ($2\theta = 18{\cdot}3$, 30·1, 35·5, 37·0, 43·2, 53·6, 57·0, 62·7 and 74·1°) at the XRD patterns of MQ[*n*] relate to their corresponding indices (111), (220), (311), (222), (400), (422), (511), (440) and (533), respectively. This indicates that MQ[*n*] is pure Fe_3O_4 with a spinal structure and it does not result in the phase change of Fe_3O_4. In addition, a small hump ($2\theta = 23$) in the XRD pattern of MQ[*n*] suggests the existence of amorphous Q[*n*] on the MQ[*n*].

The SEM images of Fe_3O_4 and MQ[*n*] are shown in figure 2. Comparing two pictures, the surface of Fe_3O_4 cube is smooth and disperse, but after combination with the Q[*n*], Fe_3O_4 cubes are loaded on the surface of cage-like Q[*n*] with high density.

FT–IR is one of the most useful tools to identify the structure of compounds. The FT–IR spectra of the Q[*n*] and MQ[*n*] are shown in figure 3, revealing the bonding of MQ[*n*] on the surface of magnetic particles. For the IR spectrum of Q[*n*], the strong peak located at 3443 cm^{-1} is crystal water of MQ[*n*], while peaks at 2930 and 1474 cm^{-1} correspond to $-CH_2$ stretching vibration and bending vibration, respectively. The characteristic absorbance band around 1722 cm^{-1} relates to the –C=O group. However, compared with the spectrum of MQ[*n*], it is notable that a new peak at 581 cm^{-1} appeared, which can be assigned to the Fe–O group. Besides, the peaks of –C=O group at 1722 cm^{-1} and $-CH_2$ stretching and bending vibrations at 2930 and 1474 cm^{-1}, which are slightly shifted to 1727, 2934 and 1478 cm^{-1}, respectively. And another peak appearing at 1631 cm^{-1} indicates that there is a weak interaction between –C=O group of Q[*n*] and Fe_3O_4, which means the generation of hydrogen bonds. The aforementioned lines of evidence indicate that Q[*n*] has been grafted successfully onto the surface of Fe_3O_4.

In order to confirm the grafting of Q[*n*] molecules onto Fe_3O_4, it is necessary to analyse the weight loss of the MQ[*n*]. As shown in figure 4, it is observed that the weight loss process can be divided into three stages during the range of temperature. The first weight loss of 11·40% below 200 °C was due to water loss adhering to the sample. The second stage occurs from 300 °C to about 600 °C, which is related to the degradation of Q[*n*]. This is a major weight loss of about 34·05% over the full temperature range. In addition, an unexpected weight loss of 19·05% appears by the end of the second stage to 800 °C, which can be characterized by the oxidation of Fe_3O_4 to Fe_2O_3. This weight loss is consistent with the amount of FeO in Fe_3O_4. Compared with the loss of organic matter of about 34·05% and the residual amount of inorganic matter about 54·55%, the composition of Q[*n*] : Fe_3O_4 in the product is ~1 : 1·5. Moreover, Q[*n*] had been modified on the surface of Fe_3O_4, which could be demonstrated by XRD and FT–IR. Therefore, the proposed structural model of MQ[*n*] is shown in figure 5.

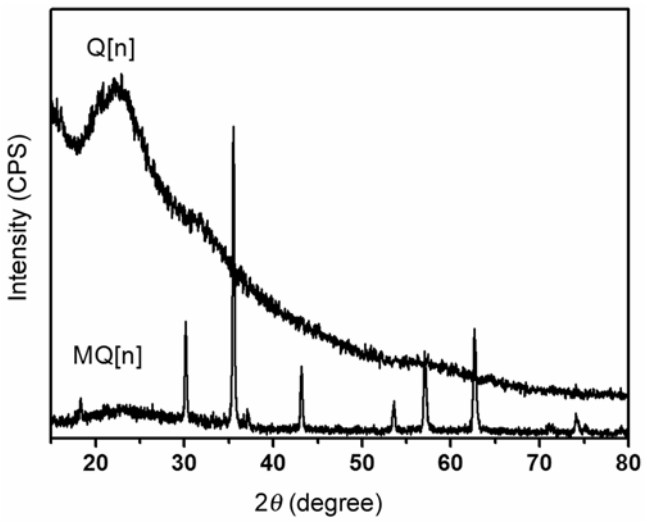

Figure 1. XRD patterns for Q[*n*] and MQ[*n*].

3.2 *Adsorption of HA onto MQ[n]*

3.2a *Effect of pH*: The pH of aqueous solution has a great influence on the HA adsorption onto MQ[*n*] and the results are illustrated in figure 6. Maximum uptake value for HA was obtained at pH 7, which was selected as optimum pH for the other experiment. HA adsorption increased with the increase of pH from 2 to 7, then dropped as pH continued to rise beyond 7. The results of the Vreysen and Maes (2008) research showed that the point of zero charge for the HA was 1·9. Therefore, the surface charge of the HA is negatively charged at the experimental conditions. However, nitrogen and carbonyl oxygen atoms on Q[*n*] are protonated at lower pH, which are favourable to adsorption. At pH above 7, less nitrogen and carbonyl oxygen atoms are protonated and more deprotonated carbonyl group could compete with negatively charged HA, thus the adsorption capacity for the HA decreases.

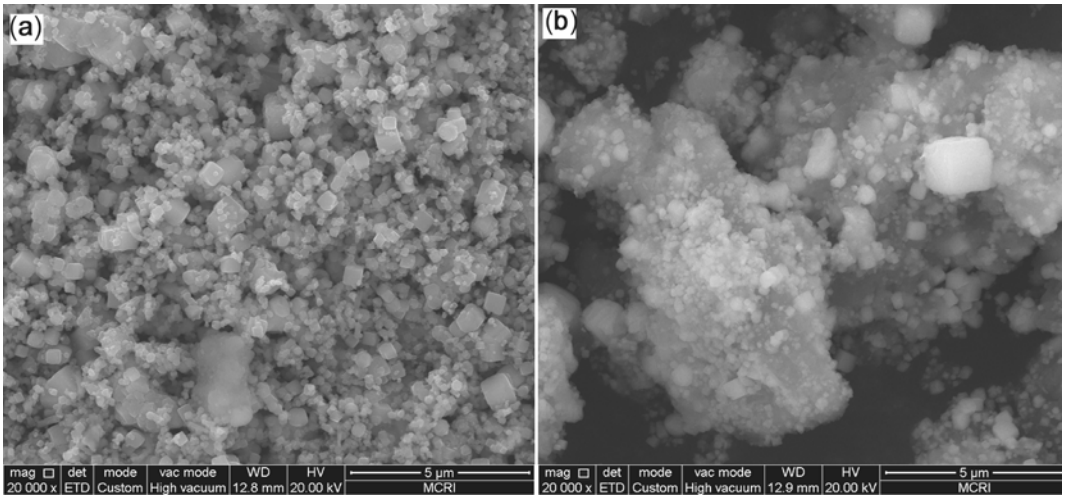

Figure 2. SEM images of Fe_3O_4 (**a**) and MQ[*n*] (**b**).

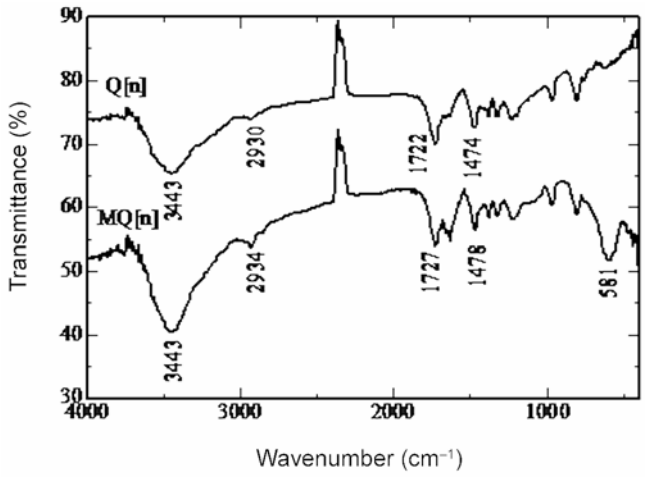

Figure 3. FT–IR spectra of Q[*n*] and MQ[*n*].

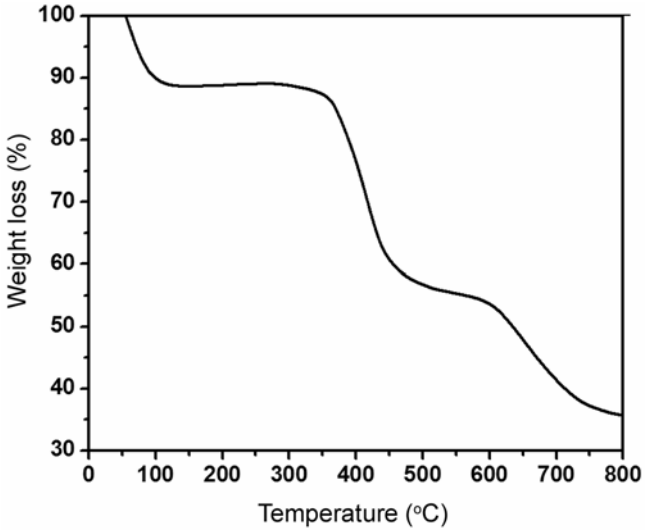

Figure 4. TGA curve of MQ[*n*].

3.2b *Adsorption isotherms*: Figure 7 displays the adsorption isotherm of HA adsorption on MQ[*n*] at 298, 308 and 318 K, respectively. The adsorption curves indicate that the equilibrium adsorption capacity of HA increases with the increase in HA concentration, but decreases with increasing temperature. In order to investigate the process of HA adsorption onto MQ[*n*], classical Langmuir isothermal adsorption theory and Freundlich equation are used, respectively, to study the adsorption mechanism (Langumuir 1918; Bayramoglu *et al* 2002).

Langmuir isothermal equation:

$$C_e/Q_e = C_e/Q_m + 1/(Q_m \cdot K_L). \quad (2)$$

Freundlich isothermal equation:

$$\ln Q_e = \ln K_F + 1/n \cdot \ln C_e, \quad (3)$$

where C_e is the equilibrium concentration of HA; Q_e the amount of adsorbed HA on a unit mass of MQ[*n*] (mg g^{-1}); Q_m the maximum adsorption (mg g^{-1}); K_L the Langmuir binding constant (L mg^{-1}), reflecting the energy of adsorption. K_F and $1/n$ are the Freundlich constants (mg g^{-1}) representing the adsorption capacity and intensity, respectively. The related parameters of Langmuir and Freundlich isotherms for HA adsorption are depicted in table 1. The maximum adsorption at 298, 308 and 318 K was calculated using Langmuir adsorption isothermal model to be 29·38, 19·10 and 14·69 mg g^{-1}, respectively, exhibiting high adsorption capacity of MQ[*n*]. However, it was significantly different from maximum adsorption obtained by linear fitting and experiment. However, the Langmuir isotherm does not fit well. $1/n$ is the isotherm constant of Freundlich adsorption isothermal model that is related to the adsorption intensity. It is acknowledged that adsorption is ideal when $0{\cdot}1 < 1/n < 0{\cdot}5$; $0{\cdot}5 < 1/n < 1$, it is easy to adsorb; $1/n > 1$, it is difficult to adsorb (Samiey and Dargahi 2010). As shown in table 1,

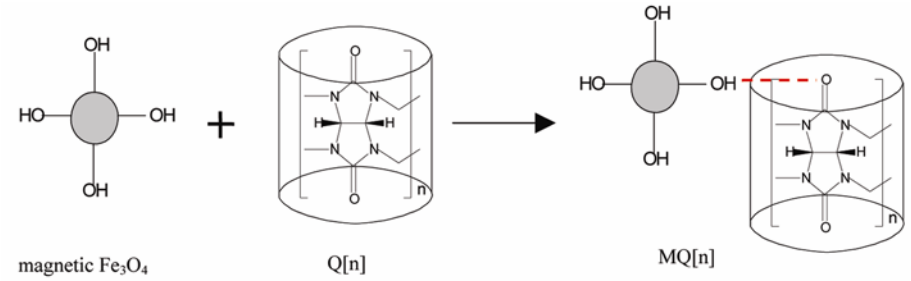

Figure 5. Schematic diagrams for the formation of MQ[*n*].

Table 1. Values of Langmuir and Freundlich constants for the adsorption of HA.

		Langmuir isotherm			Freundlich isotherm		
Adsorbent	T (K)	Q_m/(mg g^{-1})	K_L (L mg^{-1})	R^2	K_F (mg g^{-1})	1/n	R^2
HA	298	29·38	0·76	0·918	13·65	0·80	0·974
	308	19·10	0·45	0·935	5·53	0·69	0·992
	318	14·69	0·36	0·926	3·60	0·67	0·961

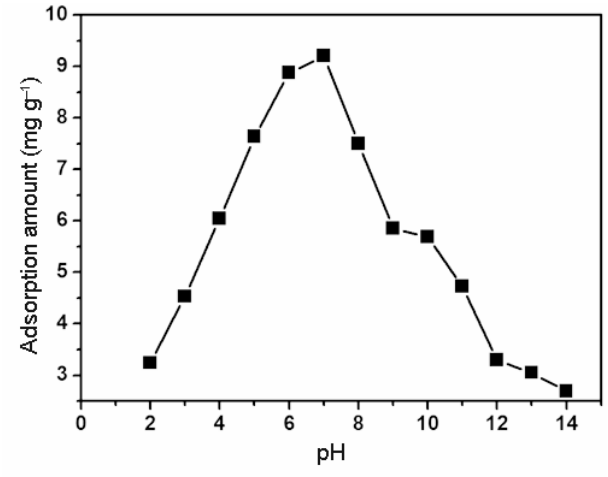

Figure 6. Effect of pH on the adsorption of HA onto MQ[*n*] at 298 K.

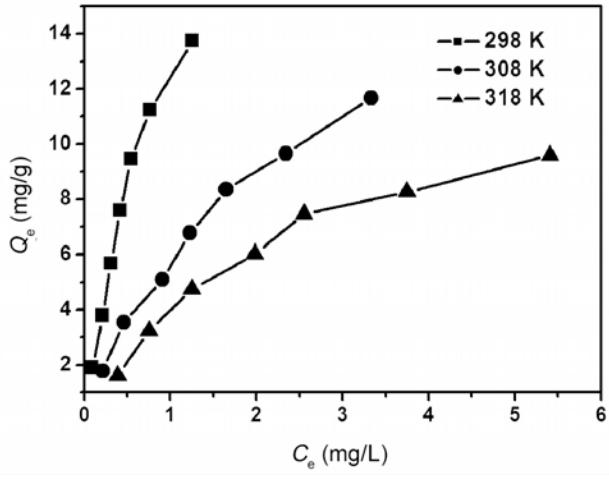

Figure 7. Adsorption isotherm of HA adsorption on MQ[*n*] at different temperatures.

the 1/*n* value of HA is between 0·6 and 0·8, indicating that HA can be easily adsorbed on the MQ[*n*]. In addition, the K_F value is increased with temperature decrease, suggesting that decrease in temperature is in favour of the adsorption. Furthermore, Freundlich isotherm fits well and correlation coefficients are better. Thus, the adsorption process is suitable for Freundlich adsorption isothermal model, which indicates that HA adsorption on MQ[*n*] is multilayer adsorption with interaction between adsorbed molecules.

3.2c *Thermodynamic parameters of adsorption*: Adsorption thermodynamic parameters can provide deeper levels of information about energy transformation in adsorption process. Thermodynamic parameters of the adsorption process such as standard free energy (ΔG^0), standard enthalpy change (ΔH^0), and standard entropy change (ΔS^0) are calculated by the following equation (Tang *et al* 2012):

$$\Delta G^0 = -RT \ln K_d, \tag{4}$$

$$\ln K_d = \Delta S^0/R - \Delta H^0/RT, \tag{5}$$

where R is the gas constant (8·314 J mol^{-1} K^{-1}) and T the absolute temperature. K_d is the equilibrium constant at temperature T. Standard free energy (ΔG^0) is calculated by (5). Plotting ln K_d vs 1/T, ΔH^0 and ΔS^0 were obtained from the slope and intercept of van't Hoff plots (figure 8). The thermodynamic data were listed in table 2.

The negative values of ΔG^0 at 288, 298 and 308 K reveal that the adsorption process is spontaneous. With the increase in temperature, ΔG^0 increases gradually and spontaneous tendency is weakened, inferring that the adsorption of HA on MQ[*n*] is difficult with increasing temperature. The negative value of ΔH^0 explains exothermic nature of adsorption process and confirms that

Table 2. Thermodynamic parameters of HA adsorption on the MQ[*n*].

Adsorbent	T (K)	$\Delta G°$/(kJ mol^{-1})	$\Delta H°$/(kJ mol^{-1})	$\Delta S°$/(J mol^{-1} K^{-1})
HA	298	–7·445		
	308	–4·439	–65·772	–197·766
	318	–2·899		

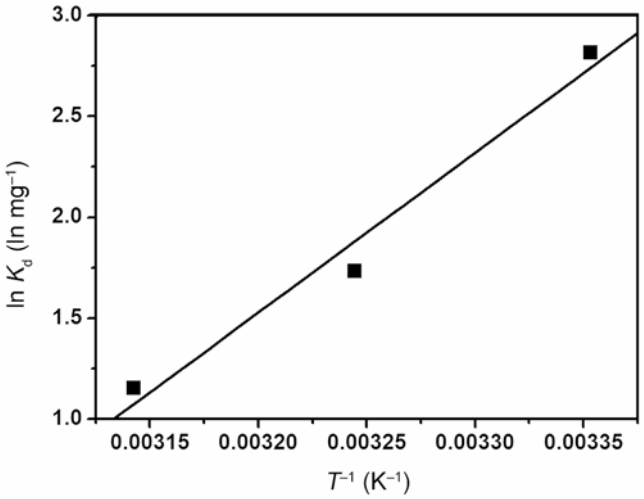

Figure 8. van't Hoff plots for the adsorption of HA on the MQ[*n*].

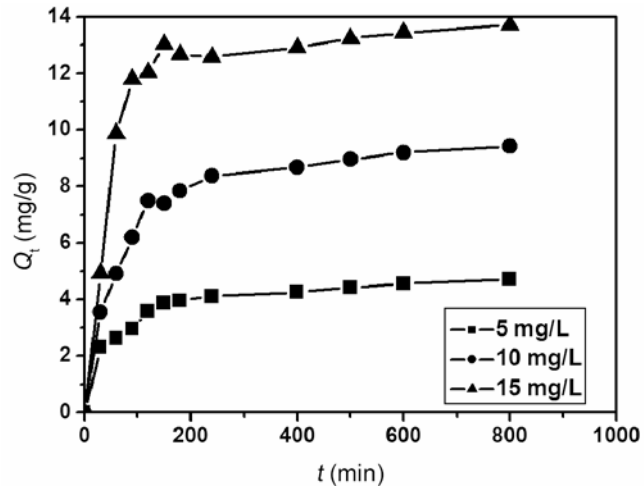

Figure 9. Adsorption kinetics of HA on MQ[*n*] at different initial concentrations.

the phenomenon of the adsorption capacity decreases as temperature increases. The negative value of ΔS^0 suggests that the entropy reduction of the adsorption process and increased randomness at the solid–solution interface. Furthermore, the value of ΔH^0 is –65·772 kJ mol^{-1}, which indicates that the adsorption process is a physico-chemical adsorption process rather than a pure physical or chemical adsorption process (Liang *et al* 2010). According to the structures of MQ[*n*] and HA, the force of adsorption process may be Van der Waals interaction, hydrophobic interaction and chemical bond force.

3.2d *Adsorption kinetics*: The adsorption kinetic curves of different initial concentration of HA adsorption onto MQ[*n*] are shown in figure 9. It is known that the three kinds of different initial concentrations of HA reach adsorption equilibrium in 12 h. The adsorption kinetics of HA on MQ[*n*] was investigated with two kinetic models, which are pseudo-first-order and pseudo-second-order models (Lagergren *et al* 1898; Ho and McKay 1998). The pseudo-first-order model is expressed as

$$\ln(Q_e - Q_t) = \ln Q_e - K_1 t, \quad (6)$$

where Q_e and Q_t are the amounts adsorbed at equilibrium time and time t (mg g^{-1}). K_1 is the rate constant of the pseudo-first-order equation (min^{-1}). The results show that the experimented data are different from those calculated, which are obtained from the linear plots. The correlation coefficients (R^2) are relatively low compared with these for pseudo-second-order model (table 3). So, the adsorption process is unsuitable for the pseudo-first-order model. The pseudo-second-order model is expressed as

$$t/Q_t = 1/K_2 Q_e^2 + t/Q_e, \quad (7)$$

where K_2 is the rate constant of the pseudo-second-order equation (g mg^{-1} min^{-1}). The values of K_2 are $5{\cdot}31 \times 10^{-3}$, $2{\cdot}40 \times 10^{-3}$ and $1{\cdot}88 \times 10^{-3}$ at different initial concentrations of HA, relating to the fast adsorption reaction ratio ($F = q_t/q_e$) and the time of arrival in F (t_F). The correlation coefficients (R^2) have high value ($R^2 > 0{\cdot}99$). In addition, the calculated maximum adsorption data are closer to the experimental data. Therefore, the pseudo-second-order model can effectively fit the adsorption process. These facts suggest that adsorption mechanism is predominant for HA adsorption to MQ[*n*] and the rate-limiting step may be a chemisorption process.

3.2e *Desorption experiments*: Desorption study was carried out to investigate the feasibility to reuse the adsorbents. Because of the low adsorption of HA on MQ[*n*] and high solubility of HA at high pH, NaOH was used to desorb the HA from MQ[*n*]. At the same time, in the basic solution, the positively charged nitrogen atoms were deprotonated and the electrostatic interaction

Table 3. Fitting parameters of HA adsorption to MQ[*n*] using pseudo-first-order and pseudo-second-order kinetic models.

		First order kinetics			Second order kinetics		
C_0 (mg g^{-1})	q_{exp} (mg g^{-1})	K_1 (min^{-1})	q_{cal} (mg g^{-1})	R^2	K_2 (g mg^{-1} min^{-1})	q_{cal} (mg g^{-1})	R^2
5	4·72	$4·67 \times 10^{-3}$	2·54	0·904	$5·31 \times 10^{-3}$	4·85	0·996
10	9·42	$5·21 \times 10^{-3}$	5·05	0·788	$2·40 \times 10^{-3}$	9·81	0·996
15	13·71	$5·42 \times 10^{-3}$	5·38	0·912	$1·88 \times 10^{-3}$	13·99	0·997

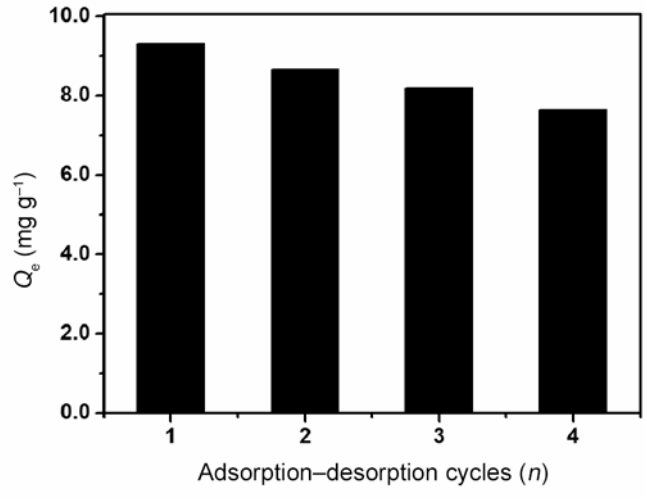

Figure 10. Adsorption amount of HA on regenerated MQ[*n*].

between MQ[*n*] and HA became much weaker. As shown in figure 10, the adsorbent amount is gradually decreased with increasing number of cycles. The adsorbent amount decreased from 9·52 to 9·31 mg g^{-1} at first cycle. After four cycles, the adsorbent amount is down to 7·64 mg g^{-1}, which is maintained up to 80% of first adsorbent amount, suggesting that MQ[*n*] has good adsorption capability and desorption property to be recycled for HA adsorption.

4. Conclusions

In this paper, MQ[*n*] was successfully synthesized with chemical co-precipitation method and the grafting of Q[*n*] molecules onto the Fe_3O_4 was confirmed by FT–IR, XRD and TGA. The adsorption studies showed that the adsorption capacity for HA depends on pH and adsorption process can be well represented by Freundlich adsorption isothermal model. The negative value of thermodynamic parameters suggested that the spontaneous and exothermic nature of adsorption process. The adsorption followed pseudo-second-order kinetics, which suggested that the limit factor of adsorption was adsorption mechanism and chemisorption process was a rate-controlling step for adsorption. In addition, MQ[*n*] could be regenerated with alkaline wash. Therefore, it has great potential to be a novel and promising adsorbent for HA.

Acknowledgements

This work is supported by the National Natural Science Foundation of China (no. 21007050), Scientific Research Program Funded by Shaanxi Provincial Education Department, China (no. 12JK0455) and the Beilin District Foundation of Xi'an of China (no. GX1205).

References

Anirudhan T S, Suchithra P S and Rijith S 2008 *Colloids Surf.* **326** 147
Baker H and Khalili F 2004 *Chim. Acta* **516** 179
Bai R B and Zhang X 2001 *J. Colloid Inter. Sci.* **243** 52
Buschmann H -J, Jansen K and Schollmeyer E 2000 *Thermochim. Acta* **346** 33
Buschmann H -J, Mutihac L and Schollmeyer E 2006 *J. Inclusion Phenom Mac. Chem.* **56** 363
Buschmann H J and Schollmeyer E 1993 *Textilveredelung* **28** 182
Bardelang D, Udachin K A and Leek D M 2007 *Cryst. Eng. Commun.* **9** 973
Bayramoglu G, Denizli A, Bektas S and Arica M 2002 *Microchem. J.* **72** 63
Domany Z, Galambos I, Vatai G and Bekassy-Molnar E 2002 *Desalination* **145** 333
Deng S and Bai R 2004 *J. Colloid Inter. Sci.* **280** 36
Feng X, Lu X J, Xue S F, Zhang Y Q, Tao Z and Zhu Q J 2009 *Inorg. Chem. Commun.* **12** 849
Ho Y and McKay G 1998 *Chem. Eng. J.* **70** 115
Ji Q, Liu H, Hu C, Qu J, Wang D and Li J 2008 *Sep. Purif. Technol.* **62** 464
Koparal A S, Yildiz Y S, Keskinler B and Demircioglu N 2008 *Sep. Purif. Technol.* **59** 175
Karcher S, Kornmüller A and Jekel Ma 2001a *Water Res.* **35** 3309
Karcher S, Kornmüller A and Jekel M 2001b *Water Res.* **35** 3317
Karcher S, Kornmüller A and Jekel M 1999 *Water Sci. Technol.* **40** 425
Latifoglu A and Gurol M D 2003 *Water Res.* **37** 1879
Lim S, Kim H, Selvapalam N, Kim K J and Cho S 2008 *Angew. Chem. Int. Ed.* **47** 3352
Langumuir I 1918 *J. Am. Chem. Soc.* **40** 1361
Liang S, Guo X Y, Feng N C and Tian Q H 2010 *J. Hazard. Mater.* **174** 756
Lagergren S 1898 *Handl* **25** 1
Peerannawar S R, Gobre V V and Gejji S P 2012 *Comput. Theor. Chem.* **983** 16

Petrov N K, Ivanov D A, Golubkov D V, Gromov S P and Alfimov M V 2009 *Chem. Phys. Lett*. **480**, 96
Parsonage P 1992 *Colloid Chem. Miner. Process.* **11** 331
Senem U C, Suphandaga S A, Kercb A and Bekboleta M 2007 *Desalination* **210** 183
Seredýnska-Sobecka B, Tomaszewska M and Morawski A W 2006 *Desalination* **198** 265
Saleh N, Al-Soud Y A, Al-Kaabi L, Ghosh I and Nau W M 2011 *Tetrahedron Lett*. **52** 5249
Samiey B and Toosi A 2010 *J. Hazard. Mater*. **184** 739
Samiey B and Dargahi M 2010 *Cent. Europ. J. Chem*. **8** 906
Tang C Y, Kwon Y N and Leckie J O 2007 *J. Membr. Sci.* **290** 86
Tang H, Zhou W J and Zhang L N 2012 *J. Hazard. Mater*. **209–210** 218
Vreysen S and Maes A 2008 *Appl. Clay Sci*. **38** 237
Wang S B and Zhu Z H 2007 *J. Coll. Interf. Sci*. **315** 41
Wang J N, Zhou Y, Li A M and Xu L 2010 *J. Hazard. Mater*. **176** 1018
Wei F, Min S, Xu L, Cheng G Z, Wu C T and Feng, Y Q 2005 *Electrophoresis* **26** 2214
Wheate N J 2008 *J. Inorg. Biochem*. **102** 2060
Yang Q, Yang Y L, Wang W D, Ge M and Li D 2012 *Adv. Mater. Res*. **413** 217
Zhao L, Luo F, Wasikiewicz J M, Mitomo H, Nagasawa N, Yagi T, Tamada M and Yoshii F 2008 *Bioresour. Technol.* **99** 1911
Zhang Y Q, Zhen L M, Yu D H, Zhao Y J, Xue S F, Zhu Q J and Tao Z 2008 *J. Mol. Struct*. **875** 435